HOLE INJECTION OXIDE BREAKDOWN MODEL FOR VERY LOW VOLTAGE LIFETIME EXTRAPOLATION

Klaus F. Schuegraf and Chenming Hu
Department of Electrical Engineering and Computer Science
University of California, Berkeley, CA 94720

Abstract - We present an anode hole injection model for silicon dioxide breakdown characterization, valid for a large thickness range between 2.5 nm and at least 13 nm, which provides a method for predicting dielectric lifetime for reduced power supply voltages and aggressively scaled oxide thicknesses. This model accurately predicts Q_{BD} and t_{BD} behavior including a fluence in excess of 10^7 C/cm^2 at V_{ox} = 2.4 V for a 2.5 nm oxide. Moreover, this model is fully complementary with the well known "thick" oxide $\frac{1}{E}$ model, while offering the ability to predict oxide reliability for low voltages.

Introduction

Future generation integrated circuits will operate in the presence of reduced supply voltages, thereby providing reduced power consumption as well as assuring adequate circuit reliability in the presence of ever increasing circuit densities. Aggressive scaling of oxide thickness appears attractive for enhancing circuit speed, thereby offsetting the disadvantage of supply voltage scaling. Concommitant high fields in the gate insulator of scaled devices pose significant reliability concerns, in particular, dielectric breakdown is a major cause of circuit failure. [1] An empirical $\frac{1}{E}$ model has been effective in formulating a procedure for the reliability assessment of dielectrics in an operating environment where supply voltages exceed 5 V. [2] However, to meet future needs of dielectric reliability assurance, a good physical understanding of thin and ultra-thin oxide breakdown at low voltages is required.

Anode Hole Injection Model

We assume a two stage breakdown process [2], divided between the time to inject a critical areal density of holes, Q_p, and a much shorter, rapid runaway process. Since the first process dictates the breakdown time, our model addresses the generation of these injected holes, as shown in Fig. 1. [3,4,5] A fraction of the

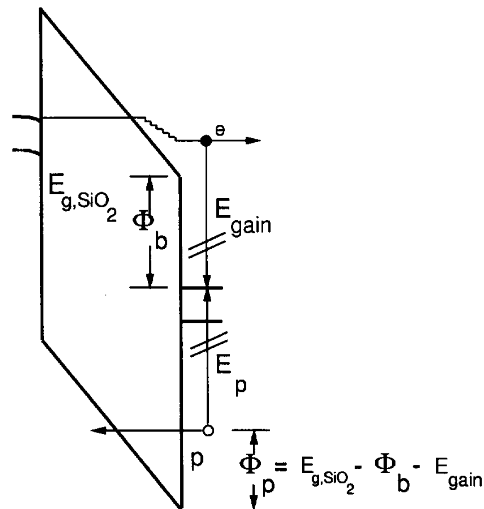

Fig. 1 Diagram of Anode Hole Injection Process. Some incident tunneling electron arrives at the anode with energy, E_{gain}, which is elastically transferred to a deep valence band electron, thereby exciting it to the lowest available energy state, that is, the anode conduction band. This excitation creates a "hot" hole capable of tunneling back into the oxide. E_{gain} is calculated by means of a phenomenological scattering model for Fowler-Nordheim Tunneling and is simply V_{ox} for Direct Tunneling.

tunneling electrons reaching the anode are able to elastically transfer their entire energy to a deep valence-band electron. Such an electron is promoted to the lowest available electron energy state, that is, the anode conduction band edge for N^+ doped poly-Si gate, thereby creating a "hot" hole, which tunnels back into the

CH3194-8/93/0000-0007$01.00 © 1993 IEEE/IRPS

oxide. These injected holes act to increase the current density at localized spots, through an as yet unspecified mechanism, which may involve the generation of interface traps [6] , bulk electron traps [7], or perhaps resonance tunneling [8], until the final electrical or thermal runaway process begins. Mathematically, the hole tunneling current is given as $J_p = \alpha_p J_n \Theta_p$, where J_n is the incident electron tunneling supply current, $\alpha_p \Theta_p$ is the probability for a hole to be generated and to tunnel through the barrier. The injected hole quantity increases with time as $J_p t$ until Q_p is reached, so that Q_{BD} is

$$Q_{BD} = \frac{J_n Q_p}{J_p} = \frac{Q_p}{\alpha_p \Theta_p} = \frac{Q_p}{\alpha_p} \exp\left(\frac{\hat{B}}{E_{ox}}\left[\Phi_p\left(V_{ox}\right)\right]^{\frac{3}{2}}\right) \quad (1)$$

$$\Phi_p = E_{g,SiO_2} - \Phi_b - E_{gain} \quad (2)$$

where $\hat{B} = 8\pi\sqrt{2m_{p,ox}} / 3q$, $m_{p,ox} = 0.295\, m_o$. The energy gained from the oxide field before arrival at the anode in the Fowler-Nordheim tunneling regime, where $V_{ox} > \Phi_b$, calculated by means of a phenomenological scattering model [9], is given as

$$E_{gain} = \Phi_b + \left(E_{ox}\lambda\right)\left[1 - \exp\left(\frac{-1}{\lambda}\left[X_{ox} - \frac{\Phi_b}{E_{ox}}\right]\right)\right], \quad V_{ox} > \Phi_b \quad (3)$$

where $\lambda = 1.5$ nm is the mean free electron scattering length in the oxide conduction band [10]. In contrast, in direct tunneling, i.e. for $V_{ox} < \Phi_b$, electrons do not experience such scattering, thus the arrival energy of electrons at the anode is simply

$$E_{gain} = V_{ox}, \qquad V_{ox} < \Phi_b. \quad (4)$$

Q_{BD} Model and Results

Intrinsic breakdown phenomena of 100 μm^2 N^+-polysilicon gate MOS test capacitors of thickness varying between 2.5 and 13 nm were studied with constant voltage stressing, recording charge to breakdown, Q_{BD}, and time to breakdown, t_{BD}, data. Fig. 2 shows the excellent agreement between this hole injection model and Q_{BD}, varying only the pre-exponential constant $\frac{Q_p}{\alpha_p}$, whose thickness dependence is given in Fig. 3. Fig. 2 underscores the power of our model, which simultaneously predicts the rapid

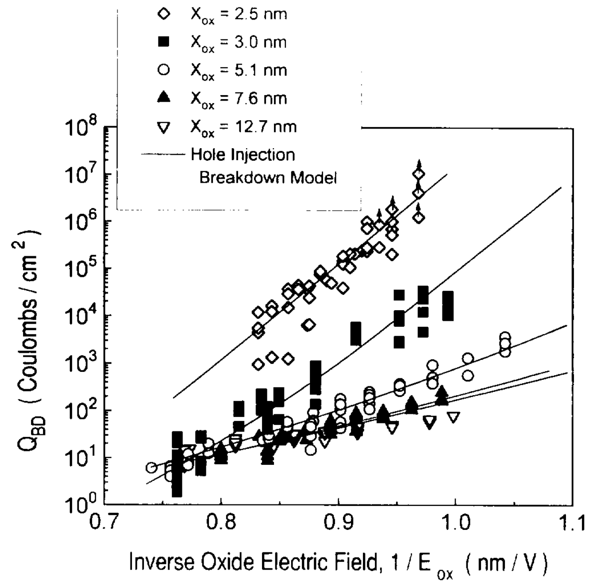

Fig. 2 Charge to Breakdown, Q_{BD}, given by Hole Injection Model compared to data measured by constant voltage stressing. Note the large increase of Q_{BD} for ultra-thin oxides compared with its fairly constant behavior for thicker oxides. The empirical $\frac{1}{E}$ model predicts a constant slope of 7.8 V/nm with respect to $\frac{1}{E_{ox}}$, coinciding with "thick" oxide data, yet failing to explain the thinner oxide result. (↑) indicates breakdown was not reached due to experimental constraints.

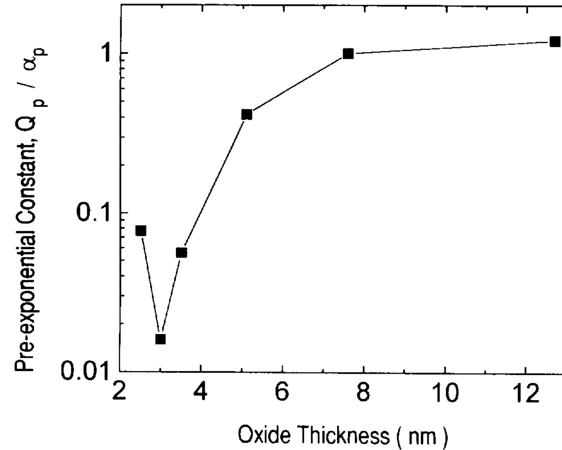

Fig. 3 Thickness variation of the pre-exponential fitting constant $\frac{Q_p}{\alpha_p}$.

increase of Q_{BD} in ultra-thin oxides, in excess of 10^7 Coul/cm^2 at $V_{ox} = 2.4$ V for $X_{ox} = 2.5$ nm, and the relatively flat field dependence of Q_{BD} for thicker oxides of 7.6 nm and 12.7 nm. Q_p measured by the technique of [11] results in Fig. 4.

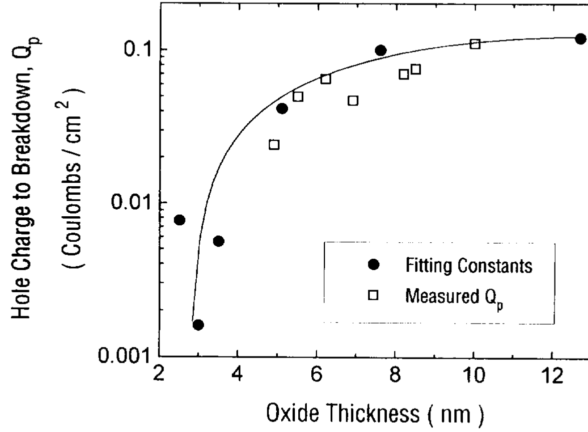

Fig. 4 Thickness dependence of Q_p, measured as in [7], coincides with Fig. 3 fitting constant when $\alpha_p \approx 0.1$.

Comparison with Fig. 3 leads to the conclusion that $\alpha_p \approx 0.1$, independent of oxide thickness; that is, the entire thickness dependence of the pre-exponential constant can be ascribed to the decrease of Q_p with oxide thickness. Fig. 4 compares Q_p data predicted by our model with Q_p measurement. Fig. 5 displays the

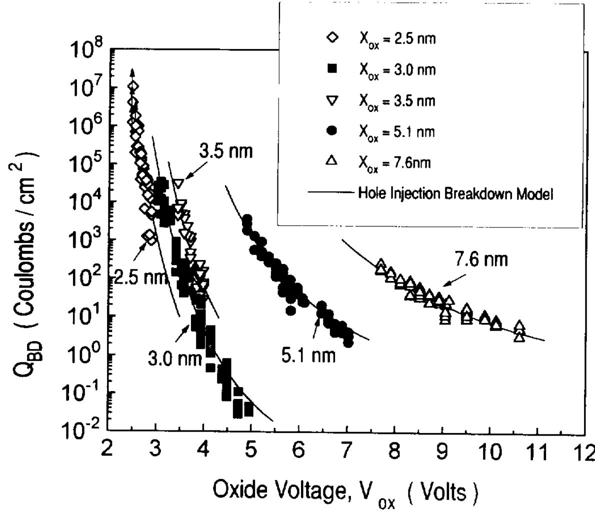

Fig. 5 Voltage dependence of Charge to Breakdown, Q_{BD}, demonstrating the ability to extrapolate to low operating voltages.

voltage dependence of Q_{BD}. The rapidly rising Q_{BD} behavior in thinner oxides can be attributed to the fact that the hot hole energy, E_{gain}, becomes more sensitive to V_{ox} when scattering becomes weaker.

Thin Oxide Conduction Model: Direct Tunneling

This section summarizes a model for tunnel current, J_n, which facilitates the modeling of t_{BD}. Fig. 6 illustrates the difference between direct and Fowler-Nordheim (FN) tunneling. The standard FN expression

$$J = A E_{ox}^2 e^{-\frac{B}{E_{ox}}}, \quad (5)$$

where $B = \frac{8\pi\sqrt{2m_{ox,n}}}{3hq}\Phi_b^{3/2}$, represents tunneling through the triangular potential barrier of Fig. 6 a, valid for $V_{ox} > \Phi_b$. We

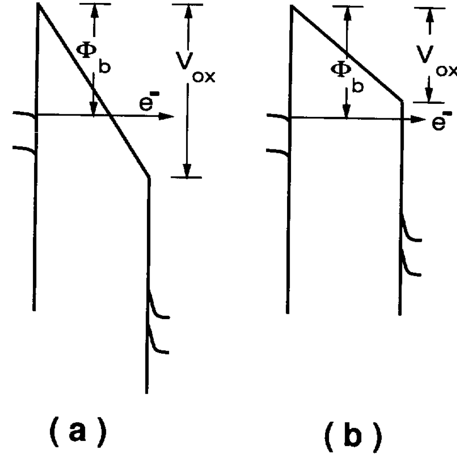

Fig. 6 Illustrates the physical difference between Fowler-Nordheim and Direct Tunneling. (a) Fowler-Nordheim Tunneling is associated with transversal of a triangular barrier. (b) Direct Tunneling is associated with transversal of a trapezoidal barrier, i.e. when $V_{ox} < \Phi_b$.

have demonstrated that the direct tunneling current, where the tunneling barrier is trapezoidal as in Fig. 6 b, Eq. (5) is increased by the following multiplicative factor for $V_{ox} < \Phi_b$ [12],

$$2\left[1-\left(\frac{V_{ox}}{2\Phi_b}\right)\right]\left(\frac{\Phi_b}{V_{ox}}\right)e^{\frac{B\left(\frac{\Phi_b - V_{ox}}{\Phi_b}\right)^{3/2}}{E_{ox}}}. \quad (6)$$

Fig. 7 demonstrates the utility of this model, highlighting the dramatic effect the changed barrier shape, from triangular to

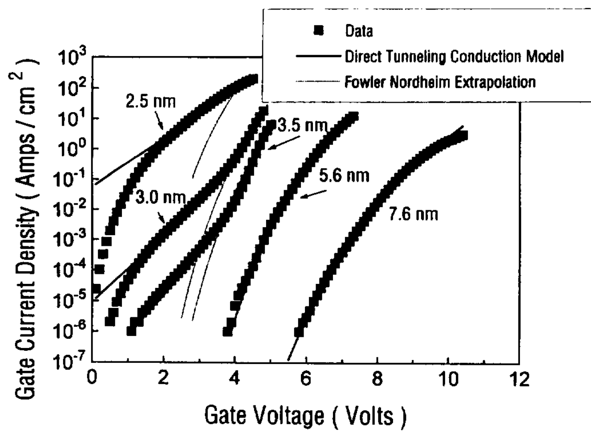

Fig. 7 Comparison between data and closed form oxide conduction current model which accounts for both Fowler-Nordheim and Direct Tunneling. The extension of Fowler-Nordheim theory for ultra-thin oxides illustrates the dramatic increase in leakage current caused by the subtle change in barrier shape, from triangular to trapezoidal, upon entering the direct tunneling regime.

trapezoidal, exerts on increasing the leakage current for $V_{ox} < \Phi_b$.

t_{BD} Model and Results

Combining this closed form current model with the Q_{BD} model expression leads to a simple model to predict oxide lifetime, i.e. $t_{BD} = \frac{Q_{BD}}{J_n}$. Fig. 8 demonstrates exceptional agreement between t_{BD} theory and data for ultra-thin oxide samples. Our model correctly accounts for the increasing lifetime acceleration slopes observed with decreasing dielectric thickness, as shown in Table I, in the framework of the empirical $\frac{1}{E}$ technique.

Thickness X_{ox} (nm)	Lifetime Acceleration Slope, G (V / nm)
3.0	65
3.5	65
5.1	49
7.6	42
12.7	36

Table I. Theoretical $\frac{1}{E}$ Extrapolation Slopes given by Anode Hole Injection Model

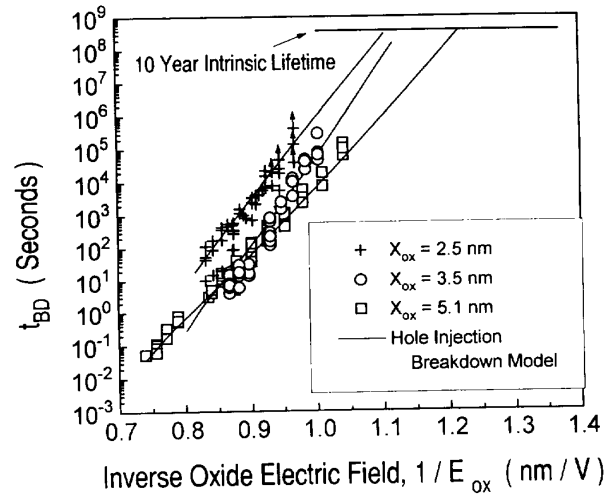

Fig. 8 Intrinsic Time to Breakdown, t_{BD}, projected by Hole Injection Model vs. $\frac{1}{E_{ox}}$. The model correctly predicts increasing lifetime acceleration slopes in thin oxides.

For example, the oft-cited 350 MV/cm "thick" oxide acceleration slope [2] appears in the 12.7 nm and thicker samples, where the electron energies are fully equilibrated by the scattering process before emission into the anode, which depends on E_{ox} rather than V_{ox}. Fig. 9 shows the result of this calculation for such a "thick",

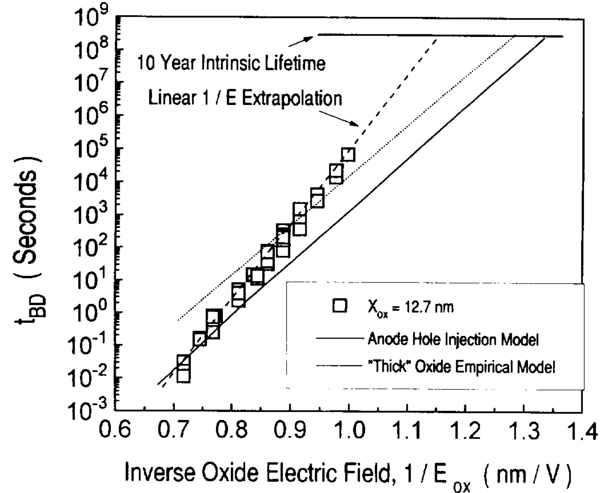

Fig. 9 Intrinsic Time to Breakdown, t_{BD}, projected by Hole Injection Model vs. $\frac{1}{E_{ox}}$, for "thick" oxide capacitor, which exhibits significant electron trapping throughout the duration of the constant voltage stress. Since the Anode Hole Injection Model accurately predicts Q_{BD} behavior, the deviation can be ascribed to the decreasing stress current. The model provides a worst-case scenario of an electron-trap-free oxide. Compare with empirical model.

12.7 nm oxide, which exhibits significant electron trapping throughout the term of the constant voltage stress. Since the model very accurately predicts the Q_{BD} behavior of this sample, we believe the deviation between measured t_{BD} data and the theoretical prediction is purely determined by electron trapping. Trapping causes the electron current to decrease with stress time, hence prolonging the breakdown time. Hence, the theoretical extrapolation paints a worst case scenario of electron-trap-free oxide; fortunately, even without correcting for electron trapping, the t_{BD} model underestimates the lifetime.

The increasing extrapolation slope appears in thin oxides, since V_{ox} begins to play a significant role in determining the arriving electron's energy. Fig. 10 demonstrates the feasibility of applying

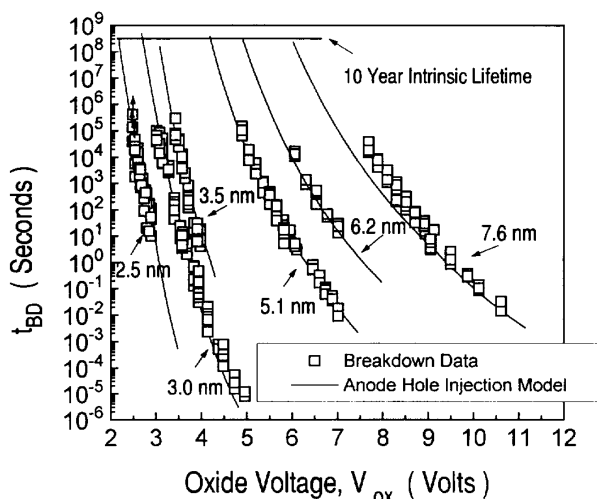

Fig. 10 Underscores the ability of the Hole Injection Model to extrapolate dielectric lifetime for low operating voltages. Note that the 2.5 nm and 3.0 nm samples both exhibit breakdown for $V_{ox} < \Phi_b$, indicating that breakdown is a continuous phenomenon even into the direct tunneling regime, a result not predicted by the empirical $\frac{1}{E}$ model.

this model in extrapolating lifetimes for low supply voltages, where the empirical model runs into conceptual difficulty because the electrons in the oxide conduction band lack sufficient energy to cause impact ionization in the oxide, the inability to account for increased acceleration slope notwithstanding.

Supply Voltage Limits

Fig. 11 examines two competing criteria, intrinsic TDDB and

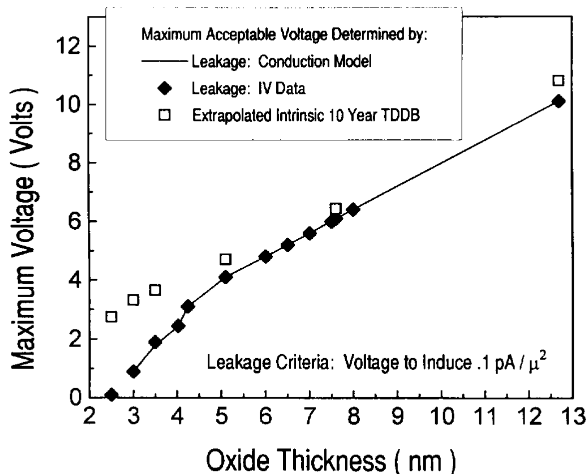

Fig. 11 Comparison of maximum acceptable operating voltages from viewpoint of 10 year intrinsic TDDB lifetime and Gate Leakage. The two criteria track each other in scaling from 13 nm to 6 nm, but further scaling leads these criteria to diverge, as the enhanced leakage current of direct tunneling mandates rapid voltage scaling. Admittedly, a more comprehensive TDDB study shows that defect TDDB rather than leakage determines supply voltage for oxide thickness greater than 7 nm; however, this qualitative trend is nevertheless expected to hold.

leakage current which influence maximum acceptable operating voltage. These two criteria track each other in scaling from 13 nm to 6 nm, but further scaling leads these criteria to diverge. Enhanced leakage current upon the transition to direct tunneling sets an additional constraint on technologies using ultra-thin oxides.

Conclusions

We have presented a new quantitative model for silicon dioxide breakdown, based on the concept of anode hole injection, valid for predicting insulator reliability performance for thicknesses between 2.5 and 12.7 nm. We believe this model is suitable in predicting dielectric lifetime for reduced supply voltages and aggressively scaled oxide thicknesses. It is a starting point for modeling defect-induced breakdown lifetime.

Acknowledgements

This research is supported by JSEP under contract DAAL-03-92-G-0242, AMD, Rockwell, and Texas Instruments under MICRO, ISTO/SDIO administered by ONR under contract N00014-85-K-0603, and SRC under contract 92-MJ-148.

References

[1] C. R. Barrett and R. C. Smith, *IEDM Technical Digest*, pp. 319-322, Dec. 1976.

[2] I. C. Chen, S. E. Holland, and C. Hu, *IEEE Trans. Elec. Dev.*, v. 32, No. 2, pp. 413 -422, Feb. 1985.

[3] Z. A. Weinberg, W. C. Hohnson, and M. A. Lampert, *Journal of Applied Physics*, v. 47, Nr. 1, pp. 248-255, No. 1, 1976.

[4] Z. A. Weinberg, M. V. Fischetti, and Y. Nissan-Cohen, *Journal of Applied Physics*, v. 59, No. 3, pp. 824-832, 1986.

[5] S. E. Holland, I. C. Chen, and C. Hu, *IEEE Elec. Dev. Let.*, v. 8, No. 12, pp. 572-575, 1987.

[6] S. K. Lai, *Journal of Applied Physics*, v. 54, No. 5, pp. 2540-2546 , 1983.

[7] I. C. Chen, S. E. Holland, and C. Hu, *Journal of Applied Physics*, v. 61, No. 9, pp. 4544-4548, 1987.

[8] B. Ricco, M. Ya. Azbel, M. H. Brodsky, *Phys. Rev. Let*, v. 51, pp. 1795-1797, 1983.

[9] C. Chang, C. Hu, and R. W. Broderson, *Journal of Applied Physics*, v. 57, No. 2, pp. 302-309, 1985.

[10] G. Lewicki and J. Maserjian, *Journal of Applied Physics*, v. 46, No. 7, pp. 3032-3039, 1975.

[11] I. C. Chen, S. E. Holland, and C. Hu, *IEDM Tech. Dig*, pp. 660-664, 1986.

[12] K. F. Schuegraf, C. C. King, and C. Hu, *Symp. VLSI Tech. Dig. of Tech. Papers*, pp. 18-19, 1992.